applied sciences

MDPI

Article

Recoil Control of Deepwater-Drilling Riser with Optimal Guaranteed Cost H_∞ Control

Yue-Ting Sun [1], Yan-Dong Zhao [1], Bao-Lin Zhang [1,*], Wei Zhang [1] and Hao Su [2]

[1] College of Automation and Electronic Engineering, Qingdao University of Science & Technology, Qingdao 266061, China; sunyt@mails.qust.edu.cn (Y.-T.S.); ydzhao@qust.edu.cn (Y.-D.Z.); zhangwqust@163.com (W.Z.)
[2] College of Information Science and Engineering, Ocean University of China, Qingdao 266100, China; suhao@ouc.edu.cn
* Correspondence: zhangbl2006@163.com

Abstract: In deepwater-drilling engineering, it is necessary to disconnect the bottom equipment of the lower marine-riser package from the blowout preventer when encountering multi-hazard environmental factors. In order to reduce the impact of recoil on the drilling platform after the sudden disconnection of the riser, in this paper, an optimal guaranteed cost H_∞ recoil control problem is considered for the drilling riser. First, a three-element mass-damper-spring deepwater-drilling riser model subject to fluid discharge and heave motion of offshore platform is given. Then, an optimal guaranteed cost H_∞ controller (OGCHC) is designed to suppress the recoil response of the drilling riser, and the sufficient conditions for the asymptotic stability of the closed-loop system are derived. Third, it is found through simulation results that the designed OGCHC can reduce the recoil response effectively. In order to further analyze the advantages of the OGCHC, the performance indices of the riser without active-recoil control and with optimal control (OC) and OGCHC are compared. It is shown that the average response amplitudes of three mass blocks of the riser are almost the same, while the control cost by the OGCHC is less than that by the OC. Further, under the designed recoil control, no riser compression occurs, thereby ensuring the safety of the riser system.

Keywords: multi-hazard; drilling riser; mud discharge; recoil control; guaranteed cost control; vibration control

Citation: Sun, Y.-T.; Zhao, Y.-D.; Zhang, B.-L.; Zhang, W.; Su, H. Recoil Control of Deepwater-Drilling Riser with Optimal Guaranteed Cost H_∞ Control. *Appl. Sci.* **2022**, *12*, 3945. https://doi.org/10.3390/app12083945

Academic Editors: Li Tian, Kaiming Bi and Chao Li

Received: 26 February 2022
Accepted: 11 April 2022
Published: 13 April 2022

1. Introduction

Typhoon, surge, wave, and earthquake generally put forward strict requirements for the safety of engineering structures [1–3]. For example, ocean current, wind, earthquake, and wave act on the deep-sea-drilling equipment for a long time, potentially leading to economic losses and pipe damage [4,5]; therefore, the drilling riser is a weak connecting part for deepwater oil and gas exploration between the submarine wellhead and the drilling ship [6–8]. The components of a deepwater-drilling riser system mainly include the drilling platform, tensioner, split joint, single riser, buoyancy joint, filling valve, lower marine-riser package (LMRP), blowout preventer (BOP), etc. In case of extreme harsh environments or dynamic-positioning failure, emergency disconnection of the LMRP and BOP is required to prevent damage to the drilling vessel [9,10].

During the disconnection operation, the deepwater-drilling riser will move upward rapidly under the tension of the tensioner and the elastic potential energy, resulting in recoil movements and endangering the safety of the drilling platform; therefore, many scholars have conducted recoil analysis on the riser, see [11–17], and the references therein. It is known that during riser emergency disconnection, the external load in the recoil process of the deepwater-drilling riser mainly comes from viscous resistance caused by discharging drilling fluid, and more and more research results concerning recoil response have been reported. In [18], the auxiliary program is used to simulate the mud column discharging

process without the filling valve. Simulation results show that the auxiliary program and the RESTEN program achieve good agreement in mud kinematic applications. In [11], an one-dimensional finite volume model is proposed to calculate the fluid pressure and velocity. In [19], a slug fluid model is established for seawater injection by the refilled valve. Based on this model, the drilling mud discharge model with a whole fluid column model is developed, where seawater and mud are considered as a whole for force analysis [20]. In [21], the friction force calculation method is introduced for slug fluid model and whole fluid column model. In particular, based on the whole fluid column model and the action force of the fluid on the riser inner wall, the drilling fluid discharge is analyzed in [15], where the drill pipe is also considered. In [22], by comparing the existing drilling mud discharge models, a more accurate three-dimension computational fluid dynamics model is developed. This shows that, to reflect practical response of drilling riser, a more accurate model of the drilling mud discharge process is required.

In recent decades, much more research attention mainly focuses on riser recoil analysis, while there are relatively few studies with regard to the riser recoil control of the drilling riser. In [23], a recoil control model of the drilling riser is proposed first, and then the linear quadratic optimal control method is proposed to control the riser recoil displacement. It is found that, under the designed optimal controller, the recoil response of the drilling riser has been reduced effectively. Note that, during the design of the optimal controller for the drilling riser, the effects of the mud discharge on the riser are not considered specifically. In fact, the classic linear quadratic optimal controller design is generally based on the known exact dynamic model, and it is not always effective to cope with uncertain systems subject to external disturbances. In other words, there still exists room for further reduction in the recoil response of the riser, which motivates our study in this paper.

Due to the existence of external disturbances and parameter perturbations, the quadratic performance index of the system with an optimal controller may generally not be minimized. In this case, one of the feasible ways is to resort to the guaranteed cost optimal control, by which a minimum upper bound of the performance index of the system may be possible. As a result, the guaranteed cost optimal control H_∞ has attracted much attention and applied in many practical applications, see references [24–30], and therein. Inspired by the above studies, in this paper, an optimal guaranteed cost H_∞ control scheme is designed to control the recoil displacement of the riser subject to friction force of fluid discharge and heave motion of the offshore platform.

The main contributions of this study are given as follows:

(i) An optimal guaranteed cost H_∞ recoil control scheme is proposed for the drilling riser system in the event of emergency disconnection. Based on this scheme, the minimum upper bound of the performance index of the riser subject to friction force of drilling fluid discharge as well as heave motion of platform can be achieved.

(ii) The existence conditions of the optimal guaranteed cost H_∞ recoil controller are derived, and the design algorithm of the recoil controller of the riser is presented. The effectiveness and advantages of the proposed active-recoil control scheme are verified through simulation results.

2. Problem Formulation

In this section, the whole fluid column model [20,23] of fluid discharge is introduced to compute the friction force of the fluid discharge on the riser. In the two cases of constant and time-varying friction coefficients, the friction force of the fluid discharge is analyzed briefly. Then, a three-element mass-damper-spring recoil control system of the drilling riser system subject to platform heave motion and fluid discharge is given. Third, an optimal guaranteed cost H_∞ recoil control problem of the drilling riser is formulated.

2.1. Whole Fluid Column Model of Fluid Discharge and Heave Motion Model of Platform

It is known that the viscous resistance of fluid discharge and the heave motion of platform have obvious effects on the recoil response of the riser. In this paper, the whole

fluid column model of fluid discharge is utilized to analyze the influence on the recoil response of the drilling riser. As stated in [20,23], the characteristics of the fluid discharge process can be described by

$$\begin{aligned}&\rho_w g A_s(L_r - L_m) + \rho_m g A_s L_m - \rho_w g A_s L_r - F_m - F_w - F_d \\ &= [\rho_w A_s(L_r - L_m) + \rho_m A_s L_m]a\end{aligned} \tag{1}$$

where

$$\begin{cases} F_m = \dfrac{f_m A_s \rho_m v^2 L_m}{2D_s}, \quad F_d = \dfrac{\rho_m A_s v^2}{2} \\ F_w = \dfrac{f_w A_s \rho_w v^2 (L_r - L_m)}{2D_s} \end{cases} \tag{2}$$

where ρ_w and ρ_m are the densities of seawater and drilling mud, respectively, kg/m^3; L_m is the length of drilling mud, m; F_m is the friction force of drilling mud, N; f_m is the friction coefficient of drilling mud; A_s is the flow area of the riser, m^2; D_s and L_r are the hydraulic diameter and the length of the riser, respectively, m; F_d is the frontal force, N; F_w is the friction force of seawater, N; f_w is the friction coefficient of seawater; v is the discharge velocity of fluid at time t, m/s; a is the acceleration of fluid at time t, m/s^2.

The drilling platform is connected to the deepwater-drilling riser by the tensioners; the heave motion of the drilling platform can be approximated as the superposition of the sine functions:

$$w(t) = \sum_{i=1}^{n} \alpha_i \sin(\omega_i t + \varphi_i) \tag{3}$$

where α_i is the random amplitude of heave motion, ω_i is the random frequency of heave motion, φ_i is the random phase of heave motion, and n is a given positive integer.

2.2. Dynamic Model of a Riser-Tension System

Notice that the tension system uses the hydraulic cylinder to drive the riser directly, and provides the required tension force for the riser. The tension force generated by a single tensioner can be calculated by [23]

$$N_t(t) = f_t - k_1 x_p - u(t) \tag{4}$$

where

$$f_t = P_{H_0} A_r - P_{L_0} A_p, \quad k_1 = \frac{\epsilon P_{H_0} A_r^2}{V_{H_0}} + \frac{\epsilon P_{L_0} A_p^2}{V_{L_0}} \tag{5}$$

with f_t representing the top tension force of the initial disconnection moment, N; P_{H_0} and P_{L_0} are the pressure of the high pressure air vessel and low pressure nitrogen vessel at the initial time, respectively, Pa; A_r and A_p are the area of piston rod side and piston rod-less side, respectively, m^2; k_1 is the spring stiffness of tensioner, N/m; ϵ is the gas constant, $\epsilon \in [1.0,\ 1.4]$; V_{H_0} and V_{L_0} are the volume of the high pressure gas and low pressure nitrogen vessel at the initial time, respectively, m^3; x_p is the displacement of piston relative to hydraulic cylinder at time t, m; $u(t)$ is the pressure drop.

Now, we aim to present a dynamic model of the riser-tension recoil control system. Similar to [15,23], the system can be simplified as a three-element mass-damper-spring model as seen in Figure 1, where m_1, m_2, and m_3 are the masses of three blocks of the whole riser, x_1, x_2, and x_3 are displacements of three mass blocks of the riser, c_1, c_2, and c_3 are the damping on the three mass blocks, k_2 and k_3 are equivalent spring stiffness of riser system with $k_2 = k_3 = EA_e/L$. E is the elastic modulus of riser, A_e is the cross-sectional area of riser, and L is the effective length of the riser.

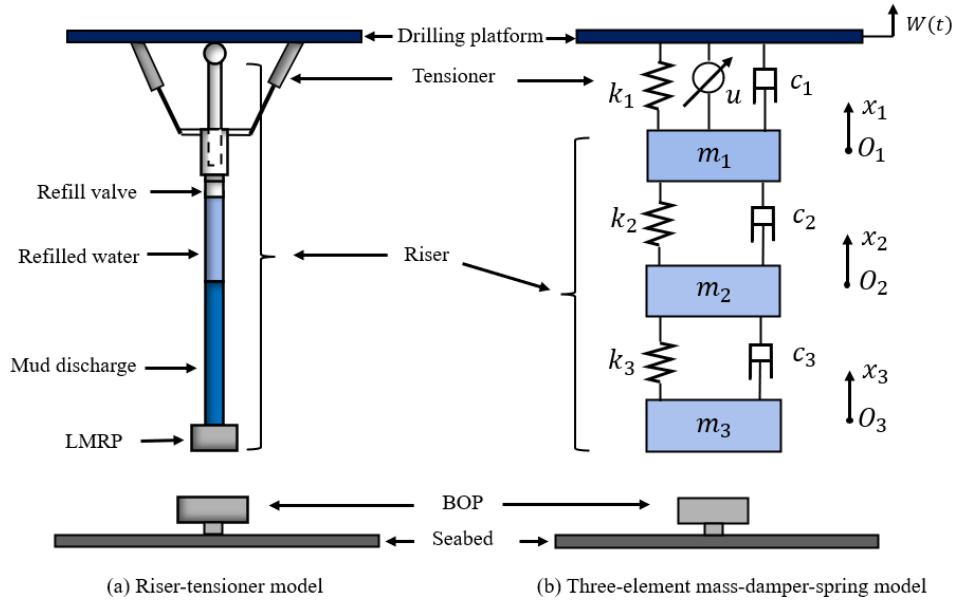

(a) Riser-tensioner model (b) Three-element mass-damper-spring model

Figure 1. A riser-tension recoil control system model. Adapted with permission from [23,31]. 2020, 2021, Elsevier.

To present dynamic equations of the riser, the following assumptions are required [15,23].

Assumption 1. *The upward direction of force and displacement is positive, and the coordinate origin of riser system is located at the position of respective initial disconnection moment.*

Assumption 2. *The influence of buoyancy modules on the riser stiffness is ignored, the drilling pipe and the riser are supposed to be concentric. The viscous resistance of drilling mud discharge is evenly distributed along the axial direction of the riser.*

Based on the Assumptions aforesaid, by Newton's second law, the dynamic equation of riser-tension control system can be expressed as

$$\begin{cases} m_1\ddot{x}_1 = -k_2(x_1 - x_2) - c_1\dot{x}_1 - c_2(\dot{x}_1 - \dot{x}_2) + N_t - F_1 \\ m_2\ddot{x}_2 = k_2(x_1 - x_2) + c_2(\dot{x}_1 - \dot{x}_2) - c_3(\dot{x}_2 - \dot{x}_3) - k_3(x_2 + x_0 - x_3) - F_2 \\ m_3\ddot{x}_3 = k_3(x_2 + x_0 - x_3) + c_3(\dot{x}_2 - \dot{x}_3) - F_3 \end{cases} \tag{6}$$

where $x_0 = (f_t - m_1 g + F_{b_1})/k_2$, and

$$\begin{cases} F_1 = F_{w_1} + F_{m_1} - F_{b_1} + m_1 g \\ F_2 = F_{w_2} + F_{m_2} - F_{b_2} + m_2 g \\ F_3 = F_{w_3} + F_{m_3} - F_{b_3} + m_3 g \end{cases} \tag{7}$$

with $F_{w_i} = F_w/3$, $F_{m_i} = F_m/3$, $i = 1, 2, 3$, and F_{b_1}, F_{b_2}, F_{b_3} representing the buoyancy during recoil of the riser.

The mass of the three blocks can be computed as

$$\begin{cases} m_1 = M_{\text{riser}}/3 + M_{\text{slip}} \\ m_2 = M_{\text{riser}}/3 \\ m_3 = M_{\text{riser}}/3 + M_{\text{LMRP}} \end{cases} \tag{8}$$

where $M_{\text{riser}} = N_b M_{\text{buoyancy}}$ is the dry weight of the riser, kg; N_b is the number of buoyancy joint; M_{buoyancy} is the dry weight of the buoyancy joint, kg; M_{slip} is the dry weight of slip joint outer cylinder, kg; M_{LMRP} is the dry weight of LMRP, kg.

The damping of the three blocks can be calculated by

$$c_1 = 0.5\sqrt{k_1 m_1},\ \ c_2 = 2\zeta\sqrt{k_2 m_2},\ \ c_3 = 2\zeta\sqrt{k_3 m_3} \tag{9}$$

where the damping ratio ζ is 0.01.

2.3. State Space Model of the Riser System and Active-Recoil Control Problem

Let

$$\begin{cases} z_1(t) = x_1(t),\ z_2(t) = \dot{x}_1(t),\ z_3(t) = x_2(t) \\ z_4(t) = \dot{x}_2(t),\ z_5(t) = x_3(t),\ z_6(t) = \dot{x}_3(t) \end{cases} \tag{10}$$

and denote $z(t) := [z_1(t)\ z_2(t)\ z_3(t)\ z_4(t)\ z_5(t)\ z_6(t)]^T$. Then, the dynamic Equation (6) can be written as

$$\dot{z}(t) = Az(t) + Bu(t) + D_1 w(t) + \tilde{D}_2 h_1(t),\ \ z(0) = z_0 \tag{11}$$

where z_0 is the system initial value as

$$z_0 = [0\ \ 0\ \ -x_0\ \ 0\ \ -x_\iota\ \ 0]^T \tag{12}$$

with $x_\iota = (f_t - m_1 g - m_2 g + F_{b_1} + F_{b_2})/k_3$, and

$$A = \begin{bmatrix} 0 & 1 & 0 & 0 & 0 & 0 \\ -\frac{k_1+k_2}{m_1} & -\frac{c_1+c_2}{m_1} & \frac{k_2}{m_1} & \frac{c_2}{m_1} & 0 & 0 \\ 0 & 0 & 0 & 1 & 0 & 0 \\ \frac{k_2}{m_2} & \frac{c_2}{m_2} & -\frac{k_2+k_3}{m_2} & -\frac{c_2+c_3}{m_2} & \frac{k_3}{m_2} & \frac{c_3}{m_2} \\ 0 & 0 & 0 & 0 & 0 & 1 \\ 0 & 0 & \frac{k_3}{m_3} & \frac{c_3}{m_3} & -\frac{k_3}{m_3} & -\frac{c_3}{m_3} \end{bmatrix},\ B = \begin{bmatrix} 0 \\ -\frac{1}{m_1} \\ 0 \\ 0 \\ 0 \\ 0 \end{bmatrix}$$

$$D_1 = \begin{bmatrix} 0 \\ \frac{k_1}{m_1} \\ 0 \\ 0 \\ 0 \\ 0 \end{bmatrix},\ \tilde{D}_2 = \begin{bmatrix} 0 & 0 & 0 \\ -\frac{1}{m_1} & 0 & 0 \\ 0 & 0 & 0 \\ 0 & -\frac{1}{m_2} & 0 \\ 0 & 0 & 0 \\ 0 & 0 & -\frac{1}{m_3} \end{bmatrix},\ h_1(t) = \begin{bmatrix} F_1 - f_t \\ F_2 + k_3 x_0 \\ F_3 - k_3 x_0 \end{bmatrix}$$

Note that the equilibrium state of the system is given by

$$\begin{cases} z_{e_1} = \dfrac{\kappa}{k_1} \\ z_{e_3} = \dfrac{\kappa}{k_1} - \dfrac{m_2 g + m_3 g - F_{b_2} - F_{b_3}}{k_2} \\ z_{e_5} = \dfrac{\kappa}{k_1} + \dfrac{\kappa}{k_2} - \dfrac{m_3 g - F_{b_3}}{k_3} \\ z_{e_2} = z_{e4} = z_{e6} = 0 \end{cases} \tag{13}$$

where $\kappa = f_t - m_1 g - m_2 g - m_3 g + F_{b_1} + F_{b_2} + F_{b_3}$.

Let

$$\tilde{z}_i(t) = z_i(t) - z_{e_i},\ i = 1, 2, \cdots, 6. \tag{14}$$

Then from (10)–(14), one yields an incremental equation of the system as

$$\dot{\tilde{z}}(t) = A\tilde{z}(t) + Bu(t) + D_1 w(t) + D_2 h(t),\ \ \tilde{z}(0) = \tilde{z}_0 \tag{15}$$

where

$$D_2 = \begin{bmatrix} 0 & -\dfrac{1}{m_1} & 0 & -\dfrac{1}{m_2} & 0 & -\dfrac{1}{m_3} \end{bmatrix}^T,\ \ h(t) = \frac{F_w + F_m}{3}$$

Let

$$\hat{h}(t) = [w^T(t),\ h^T(t)]^T,\ \ D = [D_1\ \ D_2] \tag{16}$$

Then, the system Equation (15) can be written as

$$\dot{\tilde{z}}(t) = A\tilde{z}(t) + Bu(t) + D\hat{h}(t),\ \ \tilde{z}(0) = \tilde{z}_0 \tag{17}$$

The output equation of the system is given as

$$\eta(t) = C_1\tilde{z}(t) + E_1\hat{h}(t) \tag{18}$$

where C_1 and $E_1 = [E_w\ \ E_h]$ are given matrices with appropriate dimensions.

Introducing the following quadratic performance index as

$$J = \int_0^\infty \left[\tilde{z}^T(t)Q\tilde{z}(t) + u^T(t)Ru(t)\right]dt \tag{19}$$

where the weight matrices $Q = Q^T \geq 0$ and $R = R^T > 0$.

A state feedback control law is designed as

$$u(t) = K\tilde{z}(t) \tag{20}$$

where K is a 1×6 gain matrix to be designed.

From (17) and (20), one yields the closed-loop system as

$$\dot{\tilde{z}}(t) = (A + BK)\tilde{z}(t) + D\hat{h}(t),\ \ \tilde{z}(0) = \tilde{z}_0 \tag{21}$$

The aim of this paper is to design the optimal guaranteed cost H_∞ recoil controller (20) such that

- The closed-loop system (21) with $w(t) = 0$ and $h(t) = 0$ is asymptotically stable, and $J \leq J^*$, J^* is the upper bounds of the performance;
- The H_∞ performance index

$$\|\eta(t)\| \leq \gamma\|\hat{h}(t)\| \tag{22}$$

of the closed-loop system can be guaranteed for a given $\gamma > 0$.

3. Design of Optimal Guaranteed Cost H_∞ Recoil Controller

In this section, to control the recoil responses of the riser system, an optimal guaranteed cost H_∞ control scheme is designed for the system. The existence condition and design algorithm of an optimal guaranteed cost H_∞ controller are presented for the riser recoil control system.

3.1. The Existence Condition of the Optimal Guaranteed Cost H_∞ Recoil Controller

To analyze the asymptotic stability of the closed-loop system (21), consider the following Lyapunov function as

$$V(\tilde{z}(t)) = \tilde{z}^T(t)P\tilde{z}(t) \tag{23}$$

where P is a 6×6 positive definite matrix. Then, the time derivative of $V(\tilde{z}(t))$ along system (21) is given as

$$\dot{V}(\tilde{z}(t)) = \tilde{z}^T(t)\Pi\tilde{z}(t) + 2\tilde{z}^T(t)PD\hat{h}(t) \tag{24}$$

where

$$\Pi = A^TP + K^TB^TP + PA + PBK \tag{25}$$

To prove asymptotic stability of the closed-loop system (21), set $\hat{h}(t) = 0$. Then from (24), one obtains

$$\dot{V}(\tilde{z}(t)) = \tilde{z}^T(t)(Y - Q - K^T R K)\tilde{z}(t) \tag{26}$$

where $Y = \Pi + Q + K^T R K$.

Note that

$$\dot{V}(\tilde{z}(t)) \leq \tilde{z}^T(t) Y \tilde{z}(t) - \lambda_{min}(Q + K^T R K)\|\tilde{z}(t)\|^2 \tag{27}$$

where λ_{min} represents the minimum eigenvalue of the matrix.

To guarantee the asymptotic stability of the system, we require $Y < 0$. In fact, by the Schur Complement, it is equivalent to the following matrix inequality as

$$\begin{bmatrix} \Pi & K^T R & Q \\ * & -R & 0 \\ * & * & -Q \end{bmatrix} < 0 \tag{28}$$

If the matrix inequality (28) holds, then there exists a sufficiently small positive scalar c such that $\dot{V}(\tilde{z}(t)) < -c\|\tilde{z}(t)\|^2, \tilde{z}(t) \neq 0$, which indicates that riser system (17) is asymptotically stable.

Integrating both sides of (26) from 0 to ∞, one obtains

$$\int_0^\infty \tilde{z}^T(t)(Q + K^T R K)\tilde{z}(t)dt < V(0) \tag{29}$$

That is to say, the quadratic performance index J satisfies $J < \tilde{z}^T(0) P \tilde{z}(0)$.

Then, we try to find the condition guaranteeing the H_∞ performance index (22) of the riser system. Denote

$$\beta(t) = [\tilde{z}^T(t) \;\; \hat{h}^T(t)]^T \tag{30}$$

Then, it follows from (24) and (18) that

$$\dot{V}(\tilde{z}(t)) + \eta^T(t)\eta(t) - \gamma^2 \hat{h}^T(t)\hat{h}(t) \leq \beta^T(t)\Psi\beta(t) \tag{31}$$

where

$$\Psi = \begin{bmatrix} Y + C_1^T C_1 & PD + C_1^T E_1 \\ * & -\gamma^2 I + E_1^T E_1 \end{bmatrix} \tag{32}$$

Note that $\Psi < 0$ is equivalent to the following matrix inequality as

$$\begin{bmatrix} \Pi & PD & K^T R & Q & C_1^T \\ * & -\gamma^2 I & 0 & 0 & E_1^T \\ * & * & -R & 0 & 0 \\ * & * & * & -Q & 0 \\ * & * & * & * & -I \end{bmatrix} < 0 \tag{33}$$

If the above inequality holds, then from (31), one yields

$$\dot{V}(\tilde{z}(t)) + \eta^T(t)\eta(t) - \gamma^2 \hat{h}^T(t)\hat{h}(t) < 0 \tag{34}$$

Further, integrating both sides of (34) and noticing the zero initial state condition of the system yields the H_∞ performance index inequality (22) directly.

Note that the inequality (33) implies that (28) holds, which indicates if the inequality (33) holds, then the closed-loop system (21) with $\hat{h}(t) = 0$ is asymptotically stable, the

quadratic performance index (19) is bounded, and the H_∞ performance (22) is guaranteed for the friction force $\hat{h}(t)$.

To obtain the minimum upper bound of the quadratic performance index J, introducing an upper bound $\mu > 0$, i.e., $\tilde{z}^T(0)P\tilde{z}(0) < \mu$, which is equivalent to the one as

$$\begin{bmatrix} -\mu & \tilde{z}^T(0) \\ * & -P^{-1} \end{bmatrix} < 0 \tag{35}$$

Now, we state a proposition which provides the existence of the optimal guaranteed cost H_∞ recoil controller for the riser system.

Proposition 1. *For a given scalar $\gamma > 0$, matrices $Q \geq 0$, $R > 0$, and the initial state value $\tilde{z}(0)$, if there exist 6×6 matrix $P > 0$ and 1×6 matrix K such that the inequalities (33) and (35) hold, then the optimal guaranteed cost H_∞ recoil controller (20) for the riser system (6) can be designed, and the gain matrix K of the controller is solvable.*

3.2. Computation of the Gain Matrix K of the Controller

To solve the gain matrix K of the optimal guaranteed cost H_∞ recoil controller, let

$$\Phi = \mathrm{diag}\left\{P^{-1},\ I,\ I,\ I, I\right\}$$

and pre- and post-multiply both sides of (33) by Φ and its transpose, respectively; denote $\bar{P} = P^{-1}$ and $\bar{K} = KP^{-1}$. Then, from (33) and (35), one obtains the following linear matrix inequalities as:

$$\begin{bmatrix} \bar{\Pi} & D & \bar{K}^T R & \bar{P}Q & \bar{P}C_1^T \\ * & -\gamma^2 I & 0 & 0 & E_1^T \\ * & * & -R & 0 & 0 \\ * & * & * & -Q & 0 \\ * & * & * & * & -I \end{bmatrix} < 0 \tag{36}$$

$$\begin{bmatrix} -\mu & \tilde{z}^T(0) \\ * & -\bar{P} \end{bmatrix} < 0 \tag{37}$$

where $\bar{\Pi} = \bar{P}A^T + \bar{K}^T B^T + A\bar{P} + B\bar{K}$.

Further, the computation of the gain matrix K can be formulated as the following optimization problem:

$$\begin{aligned} &\text{Minimize } \ \mu \\ &\text{s.t. (36) } \textit{and} \text{ (37).} \end{aligned} \tag{38}$$

Now, we have the following proposition.

Proposition 2. *For a given scalar $\gamma > 0$, matrices $Q \geq 0$, $R > 0$, and the initial state value $\tilde{z}(0)$, if there exist 6×6 matrix $\bar{P} > 0$ and 1×6 matrix $\bar{K}$ such that there exists the feasible solution to the optimization problem (38), then the gain matrix K of the optimal guaranteed cost H_∞ recoil controller can be solved by $K = \bar{K}\bar{P}^{-1}$.*

Remark 1. *Proposition 2 provides a method to solve the optimal guaranteed cost H_∞ recoil controller for the riser system. Compared with the classic linear quadratic optimal controller designed in [23], where the external disturbance, i.e., the characteristics of friction force of discharging fluid on the riser are not used to design the controller, while in this paper, based on the introduced H_∞ performance index, the characteristics the friction force are used to design the recoil controller. In this sense, the designed optimal guaranteed cost H_∞ controller may be better than the optimal controller to reduce the recoil response of the riser, which was verified by simulation results, and presented in the next section.*

Remark 2. *Note that there always exists physical limitations of the controller from the application point of view. By adjusting the opening $\lambda(t)$ of the recoil control valve, the flow of hydraulic oil in the tensioner can be controlled. The opening of recoil control valve $\lambda(t)$ can be written as [23]:*

$$\lambda(t) = \sqrt{\frac{\rho_d \bar{q} A_r^3 \dot{x}_p^2(t)}{2S^2|u(t)|}}, \; u(t) \neq 0 \tag{39}$$

where the density of the hydraulic oil is represented by ρ_d, kg/m^3; $\bar{q}$ is the flow resistance coefficient; S is the maximum flow area of recoil control valve port, m^2. In the next section, during the recoil controller design and application, the above relation of the control valve opening $\lambda(t)$ and the control input $u(t)$ is considered.

4. Simulation Results

In this section, in the two cases of constant and time-varying friction coefficients, the friction force of the fluid discharge is computed, respectively, and the corresponding discharge length, velocity and total friction of fluid are analyzed. Then, an optimal guaranteed cost H_∞ controller and an optimal controller adopted in [23] are designed and used to control the recoil response of the riser.

4.1. Parameters of Deepwater-Drilling Riser System

A drilling riser with a length of 1000 m and six tensioners is applied to simulation study in what follows. The system parameters of the riser are taken from [23], and the main values are given by Table 1. Based on the settings, one yields the system matrices in (17) as

$$\begin{cases} A = \begin{bmatrix} 0 & 1 & 0 & 0 & 0 & 0 \\ -47.7777 & -0.5794 & 46.9756 & 0.1315 & 0 & 0 \\ 0 & 0 & 0 & 1 & 0 & 0 \\ 51.0082 & 0.1428 & -102.0164 & -0.3116 & 51.0082 & 0.1688 \\ 0 & 0 & 0 & 0 & 0 & 1 \\ 0 & 0 & 36.5424 & 0.1209 & -36.5424 & -0.1209 \end{bmatrix} \\ B = 10^{-6} \times \begin{bmatrix} 0 \\ -2.8153 \\ 0 \\ 0 \\ 0 \\ 0 \end{bmatrix}, \; D_1 = \begin{bmatrix} 0 \\ 0.8021 \\ 0 \\ 0 \\ 0 \\ 0 \end{bmatrix}, \; D_2 = 10^{-6} \times \begin{bmatrix} 0 \\ -2.8153 \\ 0 \\ -3.0569 \\ 0 \\ -2.1900 \end{bmatrix} \end{cases}$$

Table 1. Parameters of riser system.

Parameters	Value	Parameters	Value	Parameters	Value
P_{L_0}	150,000	V_{L_0}	2.25	N_b	42
P_{H_0}	3,050,000	V_{H_0}	4.28	D_s	0.4826
M_{slip}	28,082	A_p	0.2463	ε	5×10^{-5}
M_{LMRP}	129,496	A_r	0.2048	ν_w [1]	10^{-4}
M_{buoyancy}	23,366	A_e	0.0405	ν_m [2]	1.15×10^{-6}

[1] ν_w is the viscosity of seawater. [2] ν_m is the viscosity of mud.

In the output Equation (18), the matrices C_1 and E_1 are set as

$$C_1 = \begin{bmatrix} 0.01 & 0 & 0 & 0 & 0 & 0 \\ 0 & 0 & 0.01 & 0 & 0 & 0 \\ 0 & 0 & 0 & 0 & 0.01 & 0 \end{bmatrix}, E_1 = \begin{bmatrix} 0.01 & 0.01 & 0 & 0 \\ 0.01 & 0 & 0.01 & 0 \\ 0.01 & 0 & 0 & 0.01 \end{bmatrix}$$

In (3), set $n = 6$. Then, the response of heave motion of the platform is depicted in Figure 2.

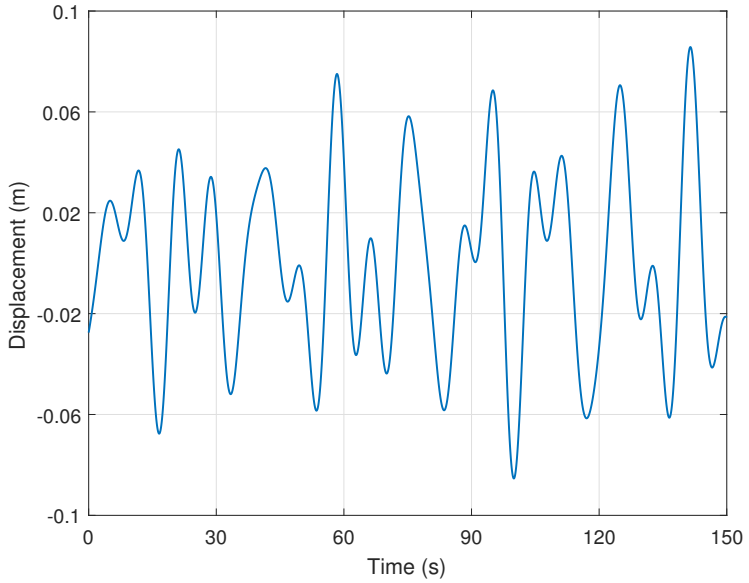

Figure 2. Response of heave motion of platform.

4.2. Analyses of the Fluid Discharge Model

Now, we compare the whole fluid column model from the length, velocity, and total friction. The two cases of constant and time-varying friction coefficients are considered, respectively.

Case I: The friction coefficients, f_w and f_m of the seawater and drilling mud, are constant. In (2), set $f_w = 0.002$ and $f_m = 0.004$; the values are taken from [23].

Case II: The fluid friction coefficients f_w and f_m are time-varying, and satisfy the Haaland formula as [21]:

$$\frac{1}{\sqrt{f_w}} = -1.8\log\left[\frac{6.9}{R_{ew}} + \left(\frac{\varepsilon}{3.7D_s}\right)^{1.11}\right] \tag{40}$$

$$\frac{1}{\sqrt{f_m}} = -1.8\log\left[\frac{6.9}{R_{em}} + \left(\frac{\varepsilon}{3.7D_s}\right)^{1.11}\right] \tag{41}$$

where ε is the roughness parameter of the riser; R_{ew} and R_{em} are the Reynolds numbers of the seawater and drilling mud, respectively.

In the above two cases, the friction force of seawater and mud discharge is computed, and the corresponding discharging time, velocity, and the total friction force of the fluid given by Table 2. It can be observed that the discharge velocity of the fluid for the time-varying friction coefficients case is slower than that for the constant case. Consequently, the overall discharge time of the fluid becomes large.

Table 2. Discharging time, velocity, and friction force of the fluid discharge under two different cases.

Case	Discharging Time (s)	Velocity (m/s^2)	Friction Force (10^5 N)
Case I	51.13	24.3094	5.6475
Case II	114.29	11.9815	8.0178

In next subsection, based on the obtained data regarding the different friction force, we investigate the anti-recoil effectiveness of the proposed optimal guaranteed cost H_∞ control scheme.

4.3. Effectiveness of the Optimal Guaranteed Cost H_∞ Controller

To design an optimal guaranteed cost H_∞ controller (OGCHC), the H_∞ performance index level γ is set as 0.55, and the weight matrices Q and R in (19) are set as

$$Q = \mathrm{diag}\{0.01,\ 0.25,\ 0.01,\ 0.25,\ 0.01,\ 0.25\},\quad R = 2.5 \times 10^{-12}$$

Then, by Proposition 2, solving the optimization problem (38) yields an OGCHC with gain matrix K as

$$K_{\mathrm{OGCHC}} = 10^5 \times \begin{bmatrix} 1.0510 & 4.0249 & -1.1883 & 1.1332 & -0.1114 & 1.4368 \end{bmatrix} \tag{42}$$

For comparison purposes, a classic optimal controller (OC) developed in [23] was designed. Set weight matrices Q and R of the linear quadratic performance index as:

$$Q = 10^4 \times \mathrm{diag}\{1,\ 1,\ 1,\ 1,\ 1,\ 1\},\quad R = 10^{-7}$$

Then the gain matrix of an OC is computed as

$$K_{\mathrm{OC}} = 10^5 \times \begin{bmatrix} -3.6435 & -4.4226 & 0.9550 & -1.8504 & -0.6362 & -2.6558 \end{bmatrix} \tag{43}$$

As the OGCHC and OC are applied to the riser system, and the controller constraint (39) is considered at the same time, the curves of the displacement responses of the three mass blocks of the riser and control force are depicted—see Figures 3–6 for the case of constant friction coefficients, and Figures 7–10 for the case of time-varying friction coefficients, respectively.

To further compare the two controllers quantitatively, the quadratic performance index of the riser system with OGCHC and OC are computed. Note that the performance index (19) are weight-matrix-dependent, and the designed OGCHC and OC are based on a different weight matrix pair, (Q, R). In this situation, the performance index (19) is modified as two weight-matrix-independent performance indices:

$$J_{\tilde{z}} = \sqrt{\frac{1}{t_f}\int_0^{t_f} \tilde{z}^T(t)\tilde{z}(t)dt} \tag{44}$$

$$J_u = \sqrt{\frac{1}{t_f}\int_0^{t_f} u^2(t)dt} \tag{45}$$

Clearly, $J_{\tilde{z}}$ and J_u are state-related and control-related root mean square values of the riser system, respectively. Denote the average displacement peak value of three mass blocks of the riser by $\hat{d}$. Then, the above indices of the riser system without control, with OC and OGCHC in the two cases of constant and time-varying friction coefficients are computed and listed in Table 3.

It can be found from Figures 3–10, and Table 3, that the controllers OGCHC and OC can reduce the recoil response of the riser system efficiently; however, the OGCHC is more economical than the OC. In fact, the average displacement amplitudes of the three mass blocks of the riser are almost the same, while the control cost by the OGCHC is less than that by the OC. In addition, the reduction in the average displacement peak value of the riser under OGCHC is larger than that under OC.

Table 3. Performance indices of the riser without control, with OC and OGCHC.

Cases	Controllers	$J_{\tilde{z}}$ (m)	$\hat{d}$ (m)	J_u (10^4 N)
I	No control	0.2362	6.2985	–
	OC [23]	0.1888	4.3066	1.0859
	OGCHC	0.1912	3.8065	1.0625
II	No control	0.3302	4.9055	–
	OC [23]	0.3001	3.6741	0.9758
	OGCHC	0.3049	2.8722	0.8956

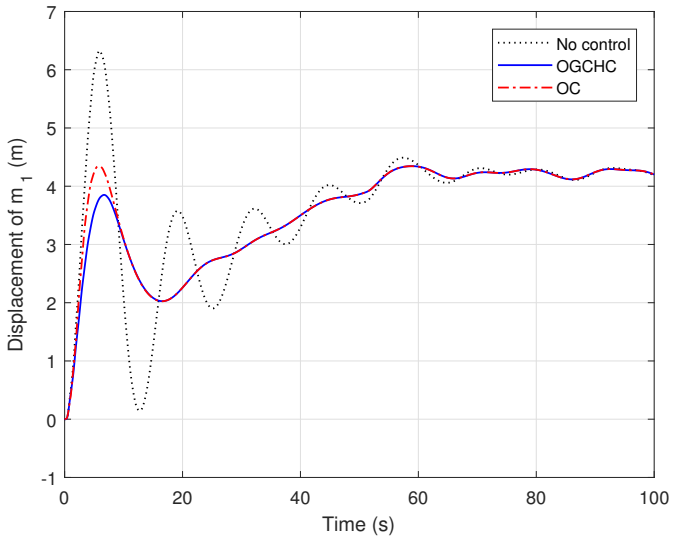

Figure 3. Displacement 1 of the riser without control, with OC and OGCHC under case I.

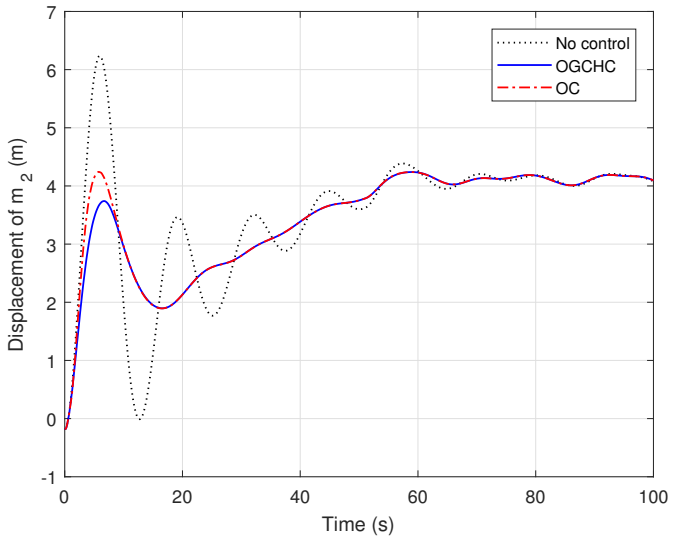

Figure 4. Displacement 2 of the riser without control, with OC and OGCHC under case I.

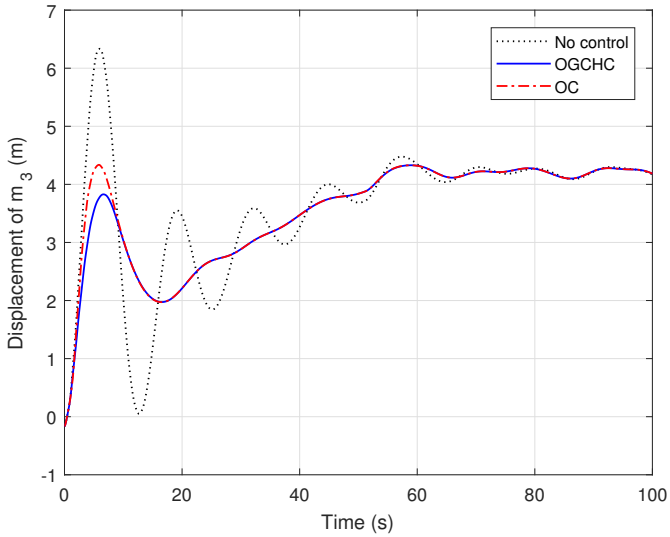

Figure 5. Displacement 3 of the riser without control, with OC and OGCHC under case I.

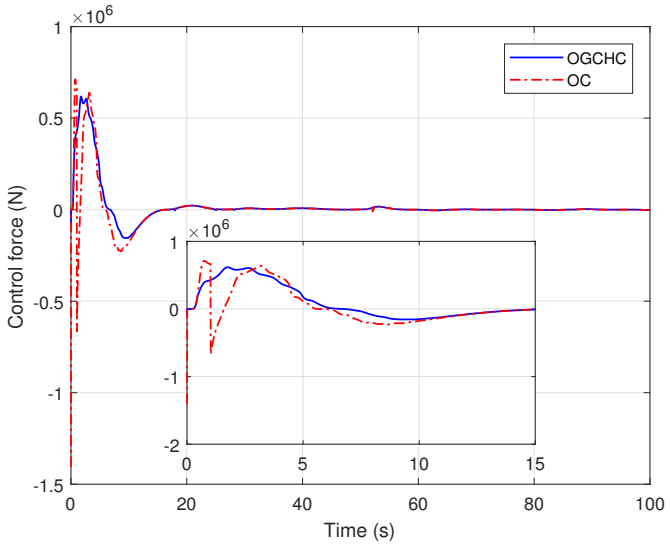

Figure 6. Control force with OC and OGCHC under case I.

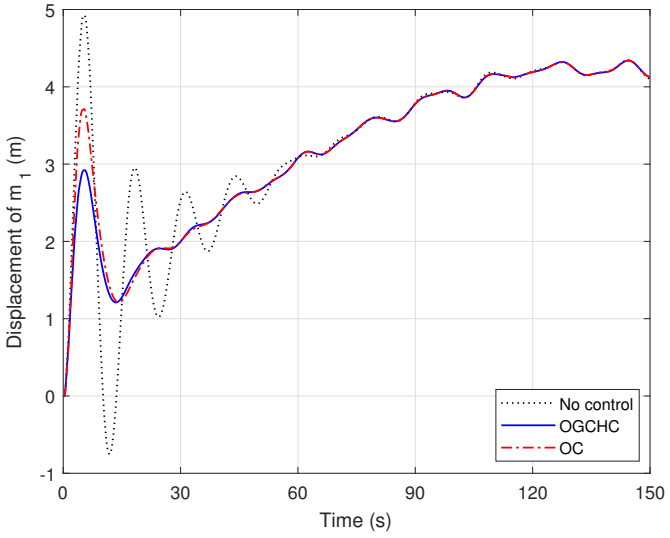

Figure 7. Displacement 1 of the riser without control, with OC and OGCHC under case II.

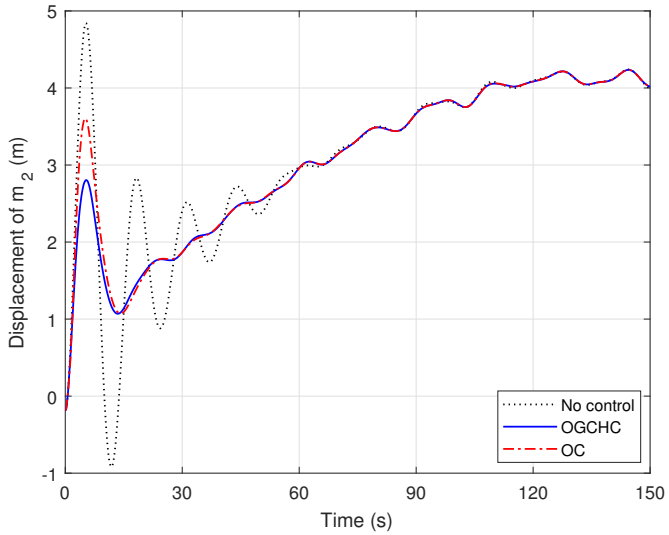

Figure 8. Displacement 2 of the riser without control, with OC and OGCHC under case II.

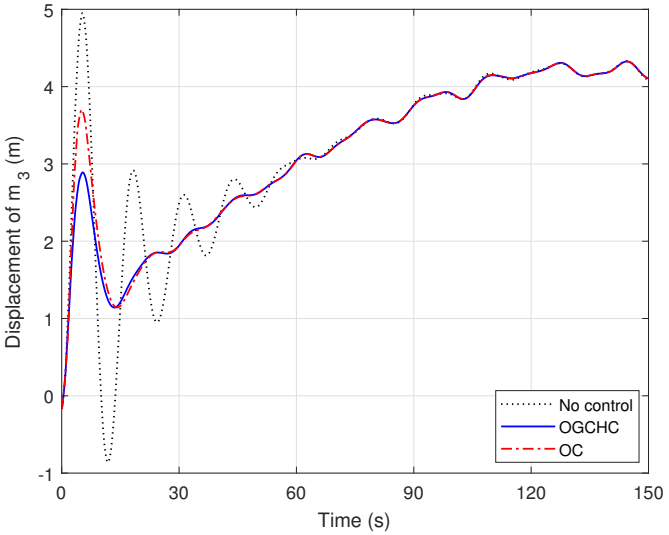

Figure 9. Displacement 3 of the riser without control, with OC and OGCHC under case II.

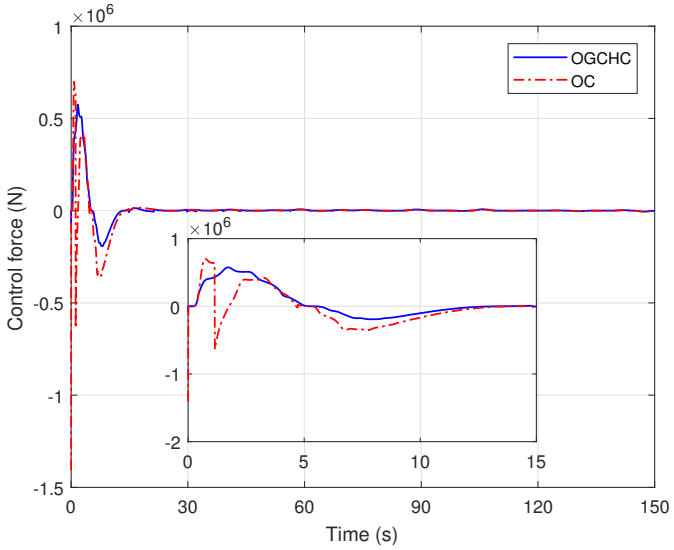

Figure 10. Control force with OC and OGCHC under case II.

Note that if the riser is compressed in the recoil process, the riser system may be collapsed. To further verify the safety of the riser under the designed recoil controller in this paper, the elongations of springs of the riser are computed. The elongation curves of the springs under the above two cases are shown in Figures 11 and 12, respectively. It can be found that the spring elongations are both greater than zero, which means that the riser is not compressed during the recoil process thereby ensuring the safety of the riser system.

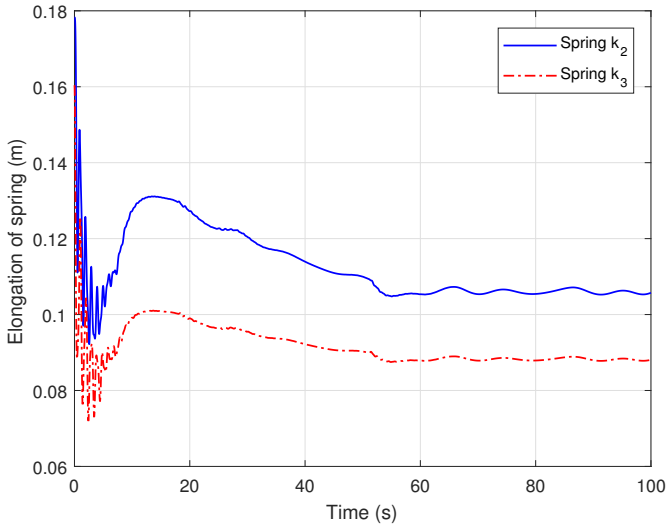

Figure 11. The elongation of springs under case I.

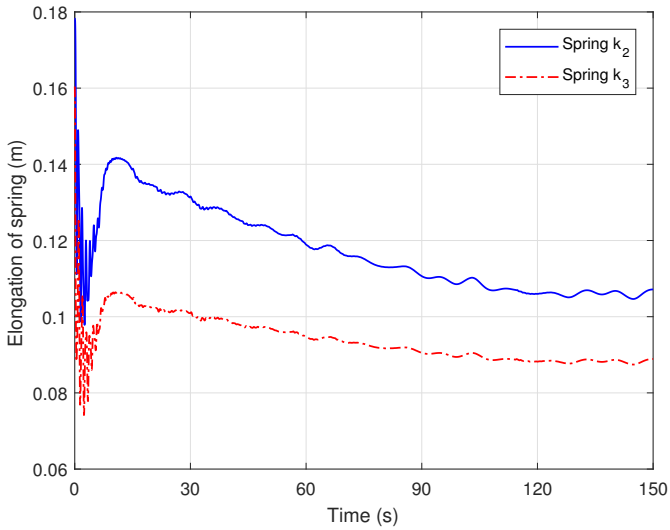

Figure 12. The elongation of springs under case II.

5. Conclusions

The recoil control issue of the deepwater-drilling riser system has been studied in this paper. First, an incremental model of the riser system has been established by considering the heave motion, linear tension force, and drilling mud discharge model. Then, an optimal guaranteed cost H_∞ recoil control scheme has been presented for the riser system, and the sufficient conditions for the asymptotic stability of the closed-loop system have been derived based on Lyapunov stability theory. In addition, under the designed recoil controller, the H_∞ performance index and the minimum upper bound of the quadratic performance index of the riser can be guaranteed.

Simulation results show that the designed optimal guaranteed cost H_∞ recoil controller is more efficient than the exiting quadratic optimal recoil controller to refrain the recoil movements of the riser. In fact, the quadratic performance index of the riser with the former

is smaller than that with the latter. It is also found that under the designed recoil controller, the compression of the riser has been avoided, and the safety of the riser has been ensured.

This paper provides an active recoil control scheme for the riser system in the event of emergency disconnection; however, there are still important issues regarding recoil analysis and control topics to be investigated in the future. It is important to further explore and understand the recoil mechanism of the riser, to provide an in-depth development potential and reasonable active-recoil control schemes.

Author Contributions: Conceptualization and methodology, B.-L.Z.; software, B.-L.Z. and Y.-T.S.; validation, Y.-D.Z., W.Z. and H.S.; formal analysis and investigation, Y.-T.S.; resources, Y.-D.Z., W.Z. and H.S.; writing—original draft preparation, Y.-T.S.; writing—review and editing, B.-L.Z.; visualization, W.Z. and H.S.; supervision, B.-L.Z. and W.Z.; project administration and funding acquisition, B.-L.Z. All authors have read and agreed to the published version of the manuscript.

Funding: This research was funded by the National Natural Science Foundation of China under Grant 61773356.

Institutional Review Board Statement: Not applicable.

Informed Consent Statement: Not applicable.

Data Availability Statement: All data presented in this paper are freely available upon request.

Conflicts of Interest: The authors declare no conflict of interest.

References

1. Li, C.; Li, H.-N.; Hao, H.; Bi, K.; Chen, B.-K. Seismic fragility analyses of sea-crossing cable-stayed bridges subjected to multi-support ground motions on offshore sites. *Eng. Struct.* **2018**, *165*, 441–456. [CrossRef]
2. Li, C.; Liu, Y.; Li, H.-N. Fragility assessment and optimum design of a steel-concrete frame structure with hybrid energy-dissipated devices under multi-hazards of earthquake and wind. *Eng. Struct.* **2021**, *245*, 112878. [CrossRef]
3. Pan, H.-Y.; Li, H.-N.; Li, C. Seismic behaviors of free-spanning submarine pipelines subjected to multi-support earthquake motions within offshore sites. *Ocean Eng.* **2021**, *237*, 109606. [CrossRef]
4. Wu, Z.; Liu, J.; Liu, Z.; Lu, Z. Parametrically excited vibrations of marine riser under random wave forces and earthquake. *Adv. Struct. Eng.* **2016**, *19*, 449–462. [CrossRef]
5. Wang, J.; Xu, L.; Cao, J.; Sheng, L.; Li, C. Numerical and experimental investigation for extreme storm-safe drilling riser. *Ship. Offshore Struc.* **2021**, 1–13. [CrossRef]
6. Chang, Y.; Chen, G.; Sun, Y.; Xu, L.; Peng, P. Nonlinear dynamic analysis of deepwater drilling risers subjected to random loads. *China Ocean Eng.* **2008**, *22*, 683–691.
7. Rocha, L.A.S.; Junqueira, P.; Roque, J.L. Overcoming deep and ultra deepwater drilling challenges. In Proceedings of the Offshore Technolog Conference, Houston, TX, USA, 5–8 May 2003; OTC-15233-MS.
8. Su, K.; Butt, S.; Yang, J.; Qiu, H. Coupled dynamic analysis for the riser-conductor of deepwater surface BOP drilling system. *Shock. Vib.* **2018**, *2018*, 6568537. [CrossRef]
9. Nguyen, D.H.; Nguyen, D.T.; Quek, S.T.; Sorensen, A.J. Position-moored drilling vessel in level ice by control of riser end angles. *Cold Reg. Sci. Technol.* **2011**, *66*, 65–74. [CrossRef]
10. Yamamoto, M.; Morooka, C.K. Feedback control system for blow-out preventer positioning. *Appl. Ocean Res.* **2019**, *82*, 362–369. [CrossRef]
11. Lang, D.W.; Real, J.; Lane, M. Recent developments in drilling riser disconnect and recoil analysis for deepwater applications. In Proceedings of the ASME 2009 28th International Conference on Ocean, Offshore and Arctic Engineering, Honolulu, HI, USA, 31 May–5 June 2009; pp. 305–318.
12. Liu, X.; Li, Y.; Zhang, N.; Sun, H.; Chang, Y.; Chen, G.; Xu, L.; Sheng, L. Improved axial dynamic analysis of risers based on finite element method and data-driven models. *Ocean Eng.* **2020**, *214*, 107782. [CrossRef]
13. Pestana, R.G.; Roveri, F.E.; Franciss, R.; Ellwanger, G.B. Marine riser emergency disconnection analysis using scalar elements for tensioner modelling. *Appl. Ocean Res.* **2016**, *59*, 83–92. [CrossRef]
14. Wang, Y.; Gao, D.; Fang, J. Axial dynamic analysis of marine riser in installation. *J. Nat. Gas Sci. Eng.* **2014**, *21*, 112–117. [CrossRef]
15. Wang, Y.; Gao, D. Recoil analysis of deepwater drilling riser after emergency disconnection. *Ocean Eng.* **2019**, *198*, 106406. [CrossRef]
16. Wang, X.; Liu, X.; Liu, Z.; Qu, N.; Hu, P.; Chang, Y.; Chen, G.; Li, C. Dynamic recoil response of tensioner and riser coupled in an emergency disconnection scenario. *Ocean Eng.* **2022**, *247*, 110730. [CrossRef]
17. Liu, X.; Liu, Z.; Wang, X.; Qu, N.; Zhang, N.; Chang, Y.; Chen, G. An intelligent recoil controller for riser system based on fuzzy control theory. *Int. J. Nav. Archit. Ocean Eng.* **2022**, *14*, 100439. [CrossRef]

18. Young, R.D.; Hock, C.J.; Karlsen, G.; Miller, J.E. Analysis and design of anti-recoil system for emergency disconnect of a deepwater riser: Case study. In Proceedings of the Offshore Technology Conference, Houston, TX, USA, 4–7 May 1992; OTC-6891-MS.
19. Grønevik, A. Simulation of Drilling Riser Deiconnection-Recoil Analysis. Master's Thesis, Norwegian Uniersity of Science and Technology, Trondheim, Norway, 2013.
20. Li, C.; Fan, H.; Wang, Z.; Ji, R.; Ren, W.; Feng X. Two methods for simulating mud discharge after emergency disconnection of a drilling riser. *J. Nat. Gas Sci. Eng.* **2016**, *28*, 142–152. [CrossRef]
21. Meng, S.; Che, C.-D.; Zhang, W.-J. Discharging flow effect on the recoil response of a deep-water drilling riser after an emergency disconnect. *Ocean Eng.* **2018**, *151*, 199–205. [CrossRef]
22. Wang, X.; Liu X.; Zhang, S.; Chen, G.; Chang, Y. Study on mud discharge after emergency disconnection of deepwater drilling risers. *J. Pet. Sci. Eng.* **2020**, *190*, 107105. [CrossRef]
23. Liu, X.; Liu, Z.; Wang, X.; Zhang, N.; Qiu, N.; Chang, Y.; Chen, G. Recoil control of deepwater drilling riser system based on optimal control theory. *Ocean Eng.* **2021**, *220*, 108473. [CrossRef]
24. Li, H.; Wang, J.; Wu, L.; Lam, H.K.; Gao, Y. Optimal guaranteed cost sliding-mode control of interval Type-2 fuzzy time-delay systems. *IEEE Trans. Fuzzy Syst.* **2018**, *26*, 246–257. [CrossRef]
25. Ye, D.; Song, T. Decentralized reliable guaranteed cost control for large-scale nonlinear systems using actor-critic network. *Neurocomputing* **2018**, *320*, 121–128. [CrossRef]
26. Wu, J.; Peng, C.; Zhang, J.; Yang, M.; Zhang, B.-L. Guaranteed cost control of hybrid-triggered networked systems with stochastic cyber-attacks. *ISA Trans.* **2020**, *104*, 84–92. [CrossRef]
27. Xie, X.; Lam, J. Guaranteed cost control of periodic piecewise linear time-delay systems. *Automatica* **2018**, *94*, 247–282. [CrossRef]
28. Zhao, Y.; Guo, G.; Ding, L. Guaranteed cost control of mobile sensor networks with Markov switching topologies. *ISA Trans.* **2015**, *58*, 206–213. [CrossRef]
29. Wu, Z.-G.; Dong, S.; Shi, P.; Su, H.; Huang, T.; Lu, R. Fuzzy-model-based nonfragile guaranteed cost control of nonlinear markov jump systems. *IEEE Trans. Syst. Man Cybern. Syst.* **2017**, *47*, 2388–2397. [CrossRef]
30. Zhang, J.; Peng, C. Guaranteed cost control of uncertain networked control systems with a hybrid communication scheme. *IEEE Trans. Syst. Man Cybern. Syst.* **2018**, *50*, 3126–3135. [CrossRef]
31. Yang, C.; Du, J.; Cheng, Z.; Wu, Y.; Li, C. Flexibility investigation of a marine riser system based on an accurate and efficient modelling and flexible multibody dynamics. *Ocean Eng.* **2020**, *207*, 107407. [CrossRef]